VCSELs with Two-Sided Beam Emission for Sensing Applications

Andreas Strodl and Rainer Michalzik

For use in optical sensors, vertical-cavity surface-emitting lasers (VCSELs) have been designed to provide simultaneous light emission from both facets. The VCSELs are based on active InGaAs quantum wells for laser output close to 960 nm wavelength where the GaAs substrate is transparent. Here we describe the laser fabrication and some static operation characteristics.

1. Introduction

VCSELs with two-sided emission have been presented in the literature long times ago (see, e.g., [1]). In the common AlGaAs material system on GaAs substrates, this is most easily achieved with the use of compressively strained InGaAs quantum wells (QWs) which have a reduced bandgap energy and with current supply through a top ring contact and a bottom ring contact at the back side of the substrate. For photon energies exceeding approximately 920 nm, the GaAs substrate is essentially transparent. For VCSELs based on GaAs QWs with emission in the 850 nm wavelength range, substrate removal or substrate replacement with, e.g., a glass wafer are alternative options. As for most cases in optical sensing, the optical pressure sensor application described in [2] requires single-mode, single-polarization emission with a high side-mode suppression ratio. In the sections to follow we first describe the chosen device structure for emission close to 960 nm wavelength and its processing and mounting and then present the experimental results for static operation. It turns out that a high-quality anti-reflection (AR) coating at the substrate side is a necessity for proper laser output.

2. VCSEL Processing and Mounting

Figure 1 shows a schematic of the selected oxide-confined VCSEL design providing simultaneous top and bottom emission. The layer structure is grown by molecular beam epitaxy on an n-type GaAs substrate. The silicon n-doped bottom distributed Bragg reflector (DBR) consists of 27.5 AlGaAs layer pairs with the Al content varying between 0 and 90 %. The one material wavelength thick active region contains three InGaAs QWs with a thickness of about 8 nm and 15 % In content. The carbon p-type doped top DBR has 24 AlGaAs layer pairs with the same composition as the n-DBR. An about 30 nm thick AlGaAs layer with almost 100 % Al content is inserted above the active region to provide current and mode confinement after selective oxidation.

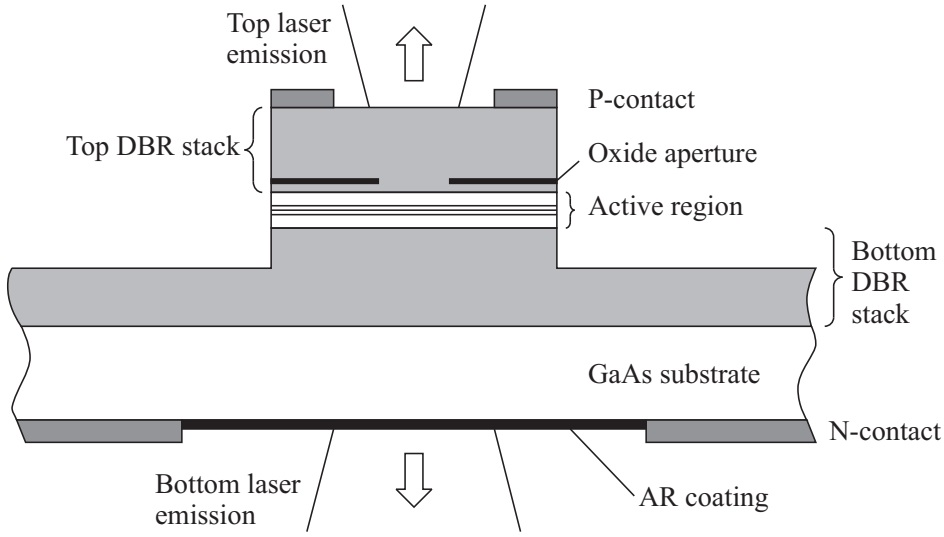

Fig. 1: Schematic cross-section of the VCSEL with two-sided emission.

VCSEL processing starts with mesa formation by wet-chemical etching, followed by selective oxidation (in a hot water vapor atmosphere) of the current aperture which defines the active diameter of the laser. The ohmic TiPtAu p-contact ring is structured with a photolithographic lift-off process. A polyimide passivation layer is then applied, onto which a NiAuTiPtAu bondpad metalization is deposited and shaped with another lift-off step. The GaAs substrate is thinned to about 180 µm to facilitate the cleaving of individual laser dies. In an annealed GeAuNiAu n-type ohmic contact at the back side of the substrate, 100 µm diameter openings centered to the active area are fabricated by lift-off for bottom light output. Finally, with another lift-off step, the openings are filled with a dielectric AR coating. The left part of Fig. 2 shows the top side view of one of the processed VCSELs. The bondpad has a width (horizontal direction) of 150 µm. The laser pitch on the sample is 250 µm.

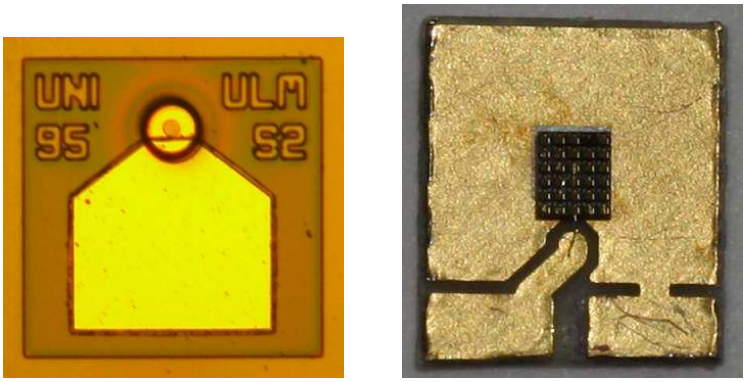

Fig. 2: Photographs of a processed VCSEL (left, top view) and of a printed-circuit board onto which a VCSEL die with 5×6 lasers has been mounted (right). The center VCSEL in the third row from the bottom is wire-bonded to the fanout track at the bottom left side of the board.

The experimental data reported in Sect. 3 were taken at wafer level by individual device probing with a contact needle. After this step, for more convenient handling, the processed sample was cleaved into individual dies of $1.25 \times 1.5\,\mathrm{mm}^2$ size containing 30 VCSELs. According to the right part of Fig. 2, such a die is soldered with indium substrate-side

down onto a small printed-circuit board from FR4 material. The large metal area on the board thus serves as the macroscopic n-contact, whereas the small metal area is connected with a bond wire to the p-bondpad of a single VCSEL in the center of the board. Underneath that VCSEL is a 400 µm diameter hole to allow bottom emission.

3. VCSEL Characterization

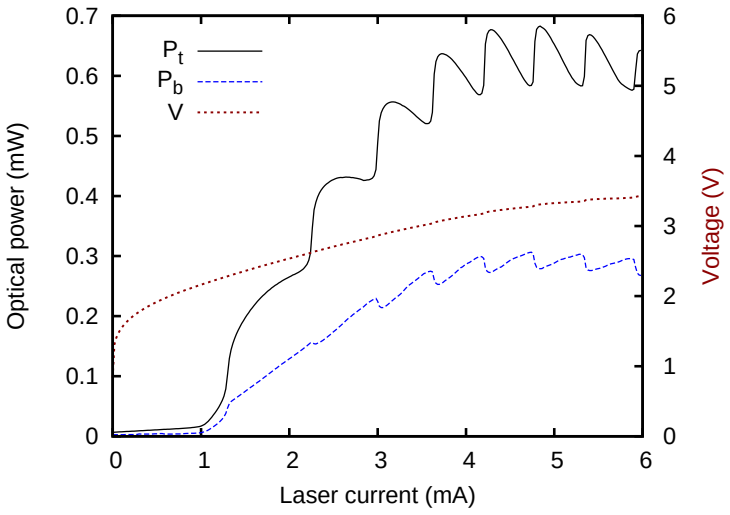

Fig. 3: LIV curves (top-emitted optical output power P_t, bottom-emitted power P_b, and voltage V versus laser current I) of a single-mode VCSEL from the first processing run.

Figure 3 shows the light–current–voltage (LIV) curves of a single-mode VCSEL with an active diameter of about 3 µm. The threshold current is a little below 1 mA. Strong ripples are seen in the LI curve for top-side emission. The ripples are less pronounced for the bottom side, and moreover the curves are anti-correlated in the sense that — at least close to thermal roll-over — local power maxima for top emission correspond to local minima for bottom emission. This VCSEL has a single quarter-wave Al_2O_3 AR coating which reduces the reflectivity of the GaAs–air interface to nominally 1.6 %. Without coating, the facet reflectivity is about 25 %, which led to even stronger power oscillations with a depth of up to 100 %.

These oscillations are caused by beam divergence and interference in the parasitic Fabry–Pérot resonator established in the GaAs substrate. Transitions between constructive and destructive interference occur due to the red-shift of the emission wavelength with increasing current at a rate of approximately 1 nm/mA. This explanation is supported by the fact that the top-side emission has a quasi-Gaussian shape over the entire current range. These VCSELs from the first processing run according to Fig. 3 were entirely unsuited for the intended application.

Obviously the reflectivity of the GaAs–air interface had to be reduced below the previous level. We have estimated a maximum tolerable reflectivity R (power reflection coefficient) of 0.1 % for proper laser operation. Experimental improvements were attempted with a dual-layer TiO_2–SiO_2 AR coating. Figure 4 illustrates the theoretical reflectivity spectrum $R(\lambda)$ of a GaAs–TiO_2–SiO_2–air layer sequence calculated for one-dimensional wave propagation. The layer thicknesses are 70 nm for TiO_2 (refractive index $n = 2.36$) and

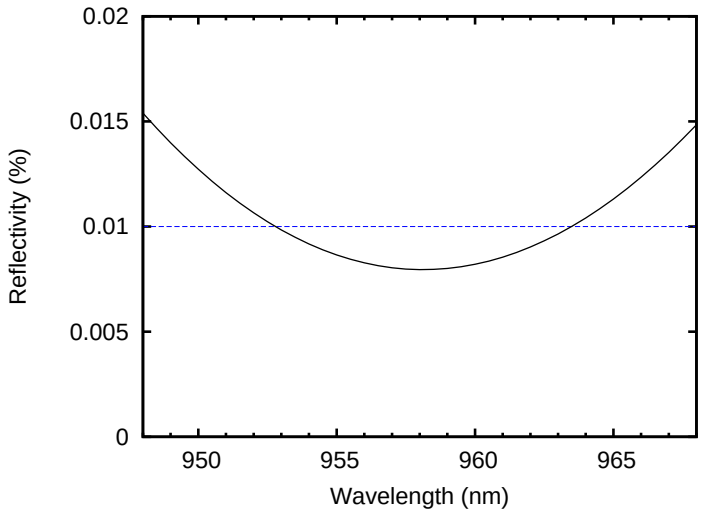

Fig. 4: Calculated reflectivity spectrum of a TiO_2–SiO_2 anti-reflection coating at the back side of the GaAs substrate.

114 nm for SiO_2 ($n = 1.49$). Close to 960 nm and over a spectral width of more than 10 nm we obtain $R < 0.01\,\%$, which is an order of magnitude lower than the target value.

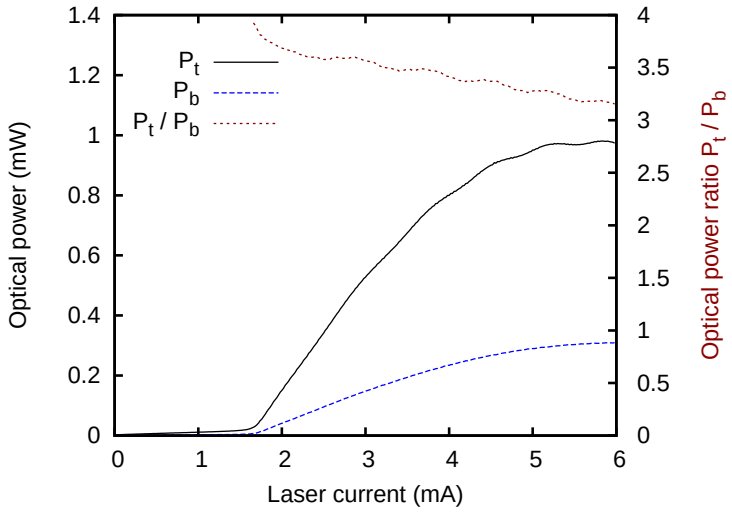

Fig. 5: Light–current characteristics $P_\mathrm{t}(I)$ and $P_\mathrm{b}(I)$ as well as the power ratio $P_\mathrm{t}(I)/P_\mathrm{b}(I)$ of a single-mode VCSEL from a second processing run with improved AR coating.

VCSEL processing was repeated for a second run, ending with the deposition of an improved dual-layer AR coating according to Fig. 4. The resulting laser output curves of a device with an active diameter of about 4 µm are displayed in Fig. 5. Compared to the laser in Fig. 3, both the threshold current and the maximum output power now have increased to about 1.7 mA and almost 1 mW, respectively. Most importantly, the power ripples have virtually vanished with some remnants remaining only in the top emission. The power outcoupling ratio is ≈ 4 at threshold and decreases to ≈ 3.2 at thermal roll-over, which might be caused by asymmetric heating of the top and bottom DBRs. A smaller power ratio would require a higher reflectivity of the top DBR, which could be achieved by deposition of dielectric material. However, this would only be a workaround involving increased processing effort. Ideally, a new VCSEL wafer with a larger number of top mirror pairs should be grown.

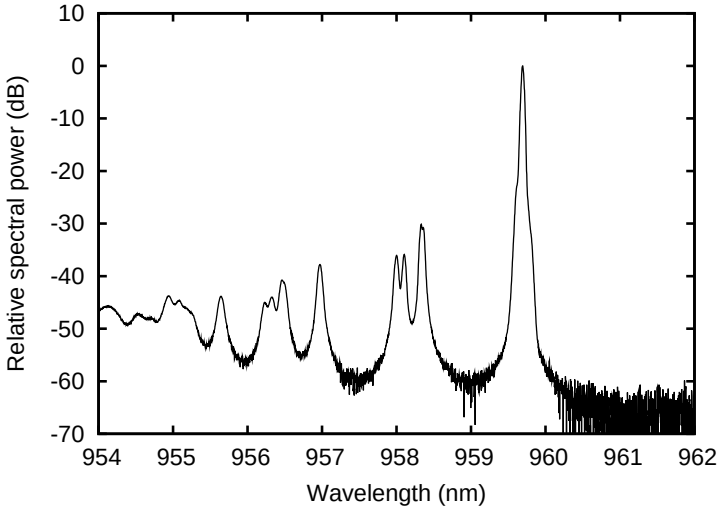

Fig. 6: Emission spectrum of the VCSEL from Fig. 5 at 5 mA current.

Figure 6 shows the emission spectrum of the laser from Fig. 5 at a current of 5 mA. It has a dominating peak at 959.7 nm wavelength which corresponds to the fundamental mode with nearly Gaussian field profile. Various higher-order transverse modes are separated by at least 1.4 nm on the short-wavelength side of the main peak. The side-mode suppression ratio is about 30 dB. Owing to the short cavity length and the associated longitudinal mode spacing in the order of 100 nm, only one longitudinal mode is able to oscillate. In other words, all transverse modes have the same longitudinal mode order. The device in Fig. 6 clearly deserves the name *single-mode VCSEL*.

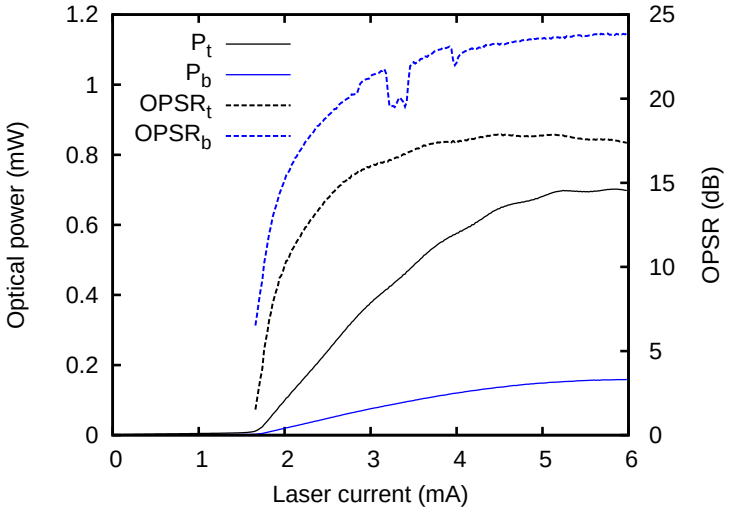

Fig. 7: LI curves repeated from Fig. 5 and corresponding OPSRs for top and bottom emission.

Since single-polarization in addition to single-mode emission is another requirement for the VCSEL sensor, the polarization properties of the lasers had also to be investigated. To reduce the processing complexity, in this initial study we did not attempt to control the light output polarization of the VCSELs, which can most favorably be done with a surface grating etched into the top DBR [3]. It is well known that standard VCSELs can show polarization switches with varying current [4]. We have taken the polarization-resolved LI curves of the VCSELs for two orthogonal directions of a polarizer inserted

in the free-space collimated beam path between the VCSEL and the photodetector. One direction coincides with the preferred polarization orientation of the device. The ratio of the two powers is called the orthogonal polarization suppression ratio (OPSR), which is usually expressed in units of decibel (dB). The top- and bottom-side OPSR curves of the VCSEL from Fig. 5 are depicted in Fig. 7 for operating currents above threshold. The laser is polarization-stable over the entire current range with a higher amount of suppression for bottom emission despite the smaller power level. Maximum OPSRs are 18 and 24 dB for top and bottom emission, respectively. The discontinuities in the curve $\mathrm{OPSR_b}(I)$ are noise artifacts at the very low power levels. It should be noted that in the literature often the peak spectral intensities are compared. This leads to larger suppression ratios because during power measurements, unpolarized spontaneous emission is added according to the large optical bandwidth of the photodetector. It must be emphasized that for a commercial low-cost use, the selection of polarization-stable devices is no option but the use of surface gratings is strongly recommended.

Acknowledgments

The authors would like to thank Rudolf Rösch and Anna Bergmann for metal deposition and substrate thinning and for various hints regarding device processing, respectively.

References

[1] G. Reiner, E. Zeeb, B. Möller, M. Ries, and K.J. Ebeling, "Optimization of planar Be-doped InGaAs VCSEL's with two-sided output", *IEEE Photon. Technol. Lett.*, vol. 7, no. 7, pp. 730–732, 1995.

[2] B. Fischer, A. Strodl, A. Hein, E. Wintner, and R. Michalzik, "VCSELs with two-sided beam emission for pressure sensor applications", in *Semiconductor Lasers and Laser Dynamics V*, K.P. Panayotov, M. Sciamanna, A.A. Valle, R. Michalzik (Eds.), Proc. SPIE 8432, paper 8432-05, 12 pages, 2012, in press.

[3] R. Michalzik, J.M. Ostermann, and P. Debernardi, "Polarization-stable monolithic VCSELs", in *Vertical-Cavity Surface-Emitting Lasers XII*, C. Lei, J.K. Guenter (Eds.), Proc. SPIE 6908, pp. 69080A-1–16, 2008.

[4] J.M. Ostermann and R. Michalzik, "Polarization Control of VCSELs", Chap. 5 in *VCSELs — Fundamentals, Technology and Applications of Vertical-Cavity Surface-Emitting Lasers*, R. Michalzik (Ed.), Springer Series in Optical Sciences, vol. 166, 33 pages. Berlin: Springer-Verlag, 2012, in press.